Chapter 14
A software platform for the analysis of porous die-cast parts using the finite cell method

Mathias Würkner, Sascha Duczek, Harald Berger, Heinz Köppe, Ulrich Gabbert

Abstract Due to the die-cast technology the manufactured parts contain unavoidable imperfections such as cavities and pores with a length scale much smaller than the size of the produced parts. Such imperfections can reduce the load bearing capacity as well as the lifetime of a part and, consequently, have to be taken into consideration during the design process. But, to include the huge amount of small scale pores in a classical finite element simulation requires an extremely refined mesh and results in a computational effort, which may exceed the capacity of todayt's computer hardware. An alternative approach is the application of the finite cell method (FCM), which can operate with non body-fitted hexahedral or tetrahedral meshes, meaning that the finite element mesh does not have to be aligned to the geometry of the structural part. The pores are taken into account in form of a STL data set (STL: standard tessellation language) coming from computed tomography (CT) or other sources, such as from a cast simulation procedure.
The paper deals with the development of a software platform, which combines the FCM with the widely used commercial finite element package Abaqus. The overall workflow along with specific implementational details are discussed. Finally, academic benchmark problems are used to verify the developed software platform.

14.1 Introduction

The development of light-weight designs in the automotive industry contributes to fulfill the EU regulations to reduce the fuel consumption as well as the carbon dioxide and nitrogen oxide emissions of combustion engines. But, also in electric vehicles the light-weight design is essential, because it contributes to an increase of the vehicle's

Mathias Würkner · Sascha Duczek · Harald Berger · Heinz Köppe · Ulrich Gabbert
Institute of Mechanics, Otto von Guericke University of Magdeburg, Universitätsplatz 2, 39106 Magdeburg, e-mail: mathias.wuerkner@ovgu.de, sascha.duczek@ovgu.de, harald.berger@ovgu.de, heinz.koeppe@ovgu.de, ulrich.gabbert@ovgu.de

H. Altenbach et al. (eds.), *Analysis and Modelling of Advanced Structures and Smart Systems*, Advanced Structured Materials 81,
https://doi.org/10.1007/978-981-10-6895-9_14

range. In general a weight reduction can be achieved by optimizing the design of the part and by changing the deployed material. The application of aluminium die-cast in connection with an optimized design fulfils the requirements for a light-weight and cost effective product. But die-cast parts show an inherent and unavoidable amount of imperfections, such as cavities and pores. A wide range of changeable parameters are available to reduce the porosity, such as a large amount of setting parameters at the die-cast machines, the thermal cycling of the manufacturing process, the amount of applied spray etc.; for details see the research results presented in (Ambos et al, 2013a).

The location, the shape, the number and the distribution of pores have a great influence on the durability and strength properties of die-cast parts. The information are available today provided by fast computed tomography (CT) scans, which are used to investigate the pore morphology in detail (Ambos et al, 2013a,b; Oberdorfer et al, 2014; Rehse et al, 2013). CT scans help to identify and to quantify the location, the size and the volume of pores. Besides the 3D coordinates of each voxel measured with a CT scan also a gray value, the so called Hounsfield scale, is assigned. From these data a STL file is derived, which represents a triangular surface tessellation, originally developed for the stereolithography process. Finally, each pore is described by a surface mesh of triangles. This topological description can be used for further steps in a finite element analysis of die-cast parts with pores. At pores high stress concentrations often occur, which may facilitate a crack initiation. Therefore, the calculation of stress concentration at the most significant pores of die-cast parts under real operating conditions is of great interest. For the overall simulation the FEM is usually used and applied to the ideal construction without regarding pores. To take into account the pores we propose to apply the finite cell method (FCM). In the following it is assumed, that the pores are given in form of a STL data set. The main difference of the FCM to the classical FEM is the concept of embedding the original or physical domain into a larger domain creating a simpler geometrical shape (Ramière et al, 2007; Saul'ev, 1963). The finite cell method (FCM) combines the so called fictitious domain approach with the FEM especially in case of higher order finite elements (Duczek et al, 2015, 2016; Düster et al, 2008; Parvizian et al, 2007; Zander et al, 2012; Rank et al, 2009).

The FCM can be interpreted as an extension of the classical FEM. If a finite element model (FE model) of the ideal geometry of a construction (without inhomogeneities such as pores) is given and additionally CT scans or STL data sets containing informations on the pore morphology are provided, the FCM can be used to calculate the stress field taking into account the real geometry of the pores. Consequently, for an industrial application it would be helpful to combine the FCM with the FEM based on commercially available software tools (Ansys, Abaqus, etc.).

The paper deals with the development of such a software platform combining the FCM with the FEM and using a STL file containing the inhomogeneities in order to calculate the displacements and stresses based on a FE model of the ideal geometry. The platform uses data interfaces and offers a flow chart, so that the complete analysis process can be performed automatically.

The paper is organized as follows. In Sect. 14.2 some basic information about the

FCM are briefly given. This also includes the main differences to the classical FEM. Then the platform concept is described in Sect. 14.3. In Sect. 14.4 some information and trouble shootings according to the STL data derived from CT measurements are discussed. In Sect. 14.5 the platform is tested by analyzing some academic test examples, which demonstrate the capability of handling the complete analysis process. The paper finishes with a summery and an outlook to further development steps.

14.2 The Finite Cell Method

Numerical methods are most preferred for solving nonlinear and complex physical problems. In engineering applications the FEM is one of the most popular methods. The basic idea of the method is to divide the physical domain of the considered problem into smaller subdomains, the so called finite elements (FEs), where in each of these domains the unknown solution is approximated by an ansatz function including a field of unknown variables, the so called degrees of freedom (DOFs). These unknowns are determined by solving a system of equations.
The finite cell method (FCM) is a numerical method, which is strongly related to the FEM. The FCM can be interpreted as an extension of the FEM and belongs to the class of fictitious domain methods (Düster et al, 2008; Parvizian et al, 2007). In the following a brief description and the fundamental equations of the FCM are presented. In addition the differences in relation to the classical FEM are emphasized. For further informations and explanations regarding the FEM and the FCM the reader is referred to other literature (Düster et al, 2008; Parvizian et al, 2007; Zienkiewicz and Taylor, 2000; Bathe, 2002; Duczek, 2014).

14.2.1 Fundamentals of the Finite Cell Method

Let us focus on a 3D problem of linear elasticity. It is assumed, that the problem is given by

$$-\operatorname{div} \underline{\underline{\tilde{\sigma}}} = \underline{f} \tag{14.1}$$

on a domain Ω. $\underline{\underline{\tilde{\sigma}}}$ denotes the second order Cauchy stress tensor. The right-hand side of the equation characterizes the body loads. Due to linear elasticity and the general use of Cartesian coordinate systems the more convenient Voigt notation is used, describing the stresses and strains in vector form. In the following vector and matrix form quantities are highlighted by a single and double underline, respectively. In order to solve a boundary value problem the boundary conditions have to be formulated. The boundary of Ω, denoted with $\partial\Omega$, is split into a Dirichlet boundary, denoted Γ_{D}, and two Neumann boundaries, denoted Γ_{N} and Γ_0. It holds $\partial\Omega = \Gamma_{\mathrm{D}} \cup \Gamma_{\mathrm{N}} \cup \Gamma_0$ and $\Gamma_{\mathrm{D}} \cap \Gamma_{\mathrm{N}} \cap \Gamma_0 = \emptyset$. The boundary conditions are given as follows

$$\underline{u} = \underline{0} \quad \text{on } \Gamma_{\mathrm{D}}, \tag{14.2}$$

$$\underline{t} = \bar{\underline{t}} \quad \text{on } \Gamma_{\mathrm{N}}, \tag{14.3}$$

$$\underline{t} = \underline{0} \quad \text{on } \Gamma_{0}, \tag{14.4}$$

where $\underline{u}$ are the displacements and $\underline{t}$ are the tractions. Adding a bar over a letter means that the quantity is prescribed. Using the Bubnov-Galerkin method the weak form of the boundary value problem is derived. Multiplying Eq. (14.1) with a test function $\underline{v}$, which is zero on the boundary Γ_{D}, and afterwards performing an integration over Ω results in a weak form of the equilibrium. Using the multidimensional integration by parts and taking into account the boundary conditions Eqs. (14.2)-(14.4) the weak form can be rewritten as

$$\int_{\Omega} \left(\underline{\underline{D}}\,\underline{v}\right)^{T} \underline{\sigma}\, d\Omega - \int_{\Gamma_{\mathrm{N}}} \underline{v}^{T} \bar{\underline{t}}\, d\Gamma - \int_{\Omega} \underline{v}^{T} \underline{f}\, d\Gamma = 0. \tag{14.5}$$

Here $\underline{\sigma}$ denotes the stresses in the Voigt notation. The quantity $\underline{\underline{D}}$ denotes the matrix of differential operators, which relates the displacements to the strains in the Voigt notation as

$$\underline{\underline{D}}\,\underline{u} = \underline{\varepsilon}. \tag{14.6}$$

Using the constitutive law of linear elasticity the weak form changes to

$$\int_{\Omega} \left(\underline{\underline{D}}\,\underline{v}\right)^{T} \underline{\underline{C}}\,\underline{\underline{D}}\,\underline{u}\, d\Omega - \int_{\Gamma_{\mathrm{N}}} \underline{v}^{T} \bar{\underline{t}}\, d\Gamma - \int_{\Omega} \underline{v}^{T} \underline{f}\, d\Omega = 0. \tag{14.7}$$

Here $\underline{\underline{C}}$ is the elasticity matrix in the Voigt notation. Instead of solving the physical problem on the original domain an expanded domain is used in the FCM, denoted with Ω_{ex} (see Fig. 14.1). The additional domain, also called fictitious domain and denoted with Ω_{fic}, is chosen in such a way, that Ω_{ex} can be characterized by a simpler geometric structure. For further investigations we assume, as shown in Fig. 14.1, that the fictitious domain is completely enclosed by the original domain. In case of

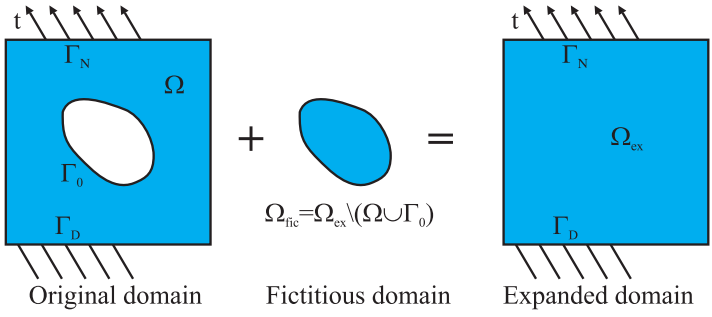

Fig. 14.1: Expansion of the original domain by a fictitious domain

investigating die-cast parts such a fictitious domain represents a pore.
Using the expansions $\underline{u}_{\text{ex}}$ and $\underline{v}_{\text{ex}}$ and additionally the continuity conditions related to displacements and tensions on the boundary $\Gamma = \partial\Omega \cap \partial\Omega_{\text{fic}}$ the weak form can be written as

$$\int_{\Omega_{\text{ex}}} \left(\underline{\underline{D}}\,\underline{v}_{\text{ex}}\right)^T \underline{\underline{C}}_{\text{ex}}\,\underline{\underline{D}}\,\underline{u}_{\text{ex}}\, d\Omega - \int_{\Gamma_{\text{N}}} \underline{v}_{\text{ex}}^T \bar{\underline{t}}\, d\Gamma - \int_{\Omega_{\text{ex}}} \underline{v}_{\text{ex}}^T \underline{f}\, d\Omega = 0. \tag{14.8}$$

Here $\underline{\underline{C}}_{\text{ex}}$ denotes the modified elasticity matrix defined by

$$\underline{\underline{C}}_{\text{ex}} = \alpha\left(\underline{x}\right)\underline{\underline{C}}, \tag{14.9}$$

where

$$\alpha\left(\underline{x}\right) = \begin{cases} 1.0 & \forall \underline{x} \in \Omega, \\ 0.0 & \forall \underline{x} \in \Omega_{\text{fic}}. \end{cases} \tag{14.10}$$

With respect to further investigations related to the numerical integration it is mentioned, that the value of α in Ω_{fic} should be replaced by a sufficiently small value representing numerical zero. This avoids severe ill-conditioning of the global stiffness matrix in the upcoming discretization process. To simplify the problem we further assume, that body loads are absent. Therefore the last term of Eq. (14.8) is neglected in further investigations.
In the FEM the domain Ω is divided into finite elements, where in the FCM the expanded domain Ω_{ex} is partitioned. Due to similarities in the discretization process of the FCM and the FEM the used elements in the FCM are currently called finite cells, which helps to distinguish between the two methods for further explanations (Düster et al, 2008; Parvizian et al, 2007). In general the finite cells differ from the classical finite elements by the fact, that they do not have to be adapted to the real physical geometry or inner boundaries, for instance caused by different material regions. This gives the opportunity to use a more simplified discretization grid. Very promising cases would be uniform grids of rectangularly shaped cells in 2D or hexahedrally shaped cells in 3D (see Fig. 14.2).
Let us just concentrate on the first term of Eq. (14.8). Assuming Ω_{ex} is completely divided into M finite cells the term can be changed to

$$\sum_{c=1}^{M} \int_{\Omega_c} \left(\underline{\underline{D}}\,\underline{v}_{\text{ex}}\right)^T \underline{\underline{C}}_{\text{ex}}\,\underline{\underline{D}}\,\underline{u}_{\text{ex}}\, d\Omega. \tag{14.11}$$

The second term can be treated in a similar way.
In similarity to the FEM the displacement $\underline{u}_{\text{ex}}$ is approximated in each cell using so called shape functions

$$\underline{u}_{\text{ex}} = \underline{\underline{N}}\,\hat{\underline{u}}. \tag{14.12}$$

Here $\underline{\underline{N}}$ and $\hat{\underline{u}}$ are the matrix of shape functions and the vector of unknown variables, the so called DOFs, respectively. Using $\underline{v}_{\text{ex}} = \underline{\underline{N}}\,\hat{\underline{v}}$, Eqs. (14.11) and (14.12) the

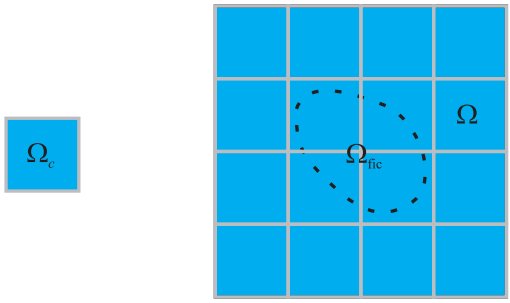

Fig. 14.2 Uniform finite cell grid of an expanded 2D domain consisting of quadratically shaped cells (right side of the figure); the occupied domain of the c-th finite cell is denoted by Ω_c (left side of the figure)

following system of equations can finally be derived for each finite cell

$$\underline{\underline{K}}\,\underline{\hat{u}} = \underline{F}. \tag{14.13}$$

By assembling the system of equations of all finite cells the global system of equations is derived as

$$\underline{\underline{K}}^{\mathrm{A}}\,\underline{\hat{u}}^{\mathrm{A}} = \underline{F}^{\mathrm{A}}. \tag{14.14}$$

The FCM is an extension of the FEM, which gives the opportunity of defining a compatible finite cell for each finite element. This also assures the possibility of creating a hybrid mesh consisting of both finite elements and finite cells. In the following such a mesh is called FE-FC mesh.

14.2.2 Numerical Integration

For the evaluation of $\underline{\underline{K}}$ and $\underline{F}$ in Eq. (14.13) integrals have to be calculated. In the classical FEM, due to mapping transformations using a reference element, the integrand is in general non-polynomial. The integration cannot be analytically performed in most of the cases. Therefore, numerical integration methods are used. For common finite elements as in commercial software tools (Abaqus, Ansys, etc.) the Gaussian quadrature is applied. This approach converges fast for sufficiently smooth integrands, but not for discontinuous ones. Referring to Fig. (14.2) and Eq. (14.11), for the finite cells the integrand is discontinuous due to the jump in the elasticity matrix. That is why in the FCM an adaptive integration scheme is used in order to capture this discontinuity in an appropriate way.
In the following, the case of discontinuous material properties is discussed. This means, the cell contains the joint boundary of the fictitious and the original domain. A common Gaussian quadrature for solving the integrals would be an inappropriate approach. Instead a composed integration is used. This integration procedure is characterized by subdividing the domain of the cell, using a subdivision scheme. In the following a quadtree subdivision procedure for the 2D case will be explained. Referring to Fig. 14.3 it is assumed, that a cell is cut by the boundary of the region.

The subdivision level, denoted with k, is zero at the beginning. For $k = 1$ the domain of the cell is split into four equal-sized subdomains, which are called subcells in the following. In order to establish the level $k = 2$ each of the four subcells is checked, whether it contains the boundary or not. If it is true the domain of the subcell is split further into four smaller subcells. In Fig. 14.3 the subcells, which have to be divided, are marked with a gray color filling. Higher subdivision levels are obtained by following the previously explained procedure until the integration is converged. In case of 3D finite cells an octree-subdivision scheme is used. Here the cells are split into eight subcells. Detailed information, such as the integration weights and points of the Gaussian quadrature, can be taken from Duczek (2014).

14.3 Concept of the Software Platform

For developing the software platform concept the programming software tool Matlab is used. The platform combines the FCM and the interaction of its interface to an appropriate commercial software tool in order to establish a complete workflow of creating the FC model, solving the problem and evaluating its strains and stresses. In this regard the programming of the platform is split into three sections. These are the preprocessor, the solver and the post processor (see Fig. 14.4).
The preprocessor deals with the creation of the FC model. In the following it is assumed, that a sample of an ideal die-cast part (without pores) is already given as a FE model and the information of the pores are separately provided in form of a STL data set. This data set contains the topology of the surface triangulation of the pores as well as the locations of the corner vertices of the triangles. The mesh of the FE model is used to perform the FC discretization. The finite elements are replaced

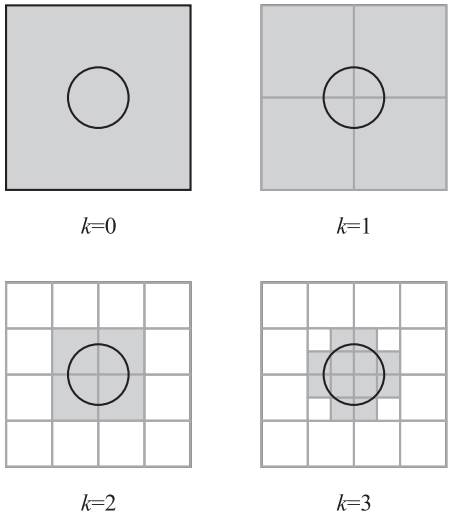

Fig. 14.3 Schematic sketch of a quadtree subdivision procedure, where the fictitious domain is represented by a circular region; cells/subcells containing at least parts of this region are highlighted in light gray

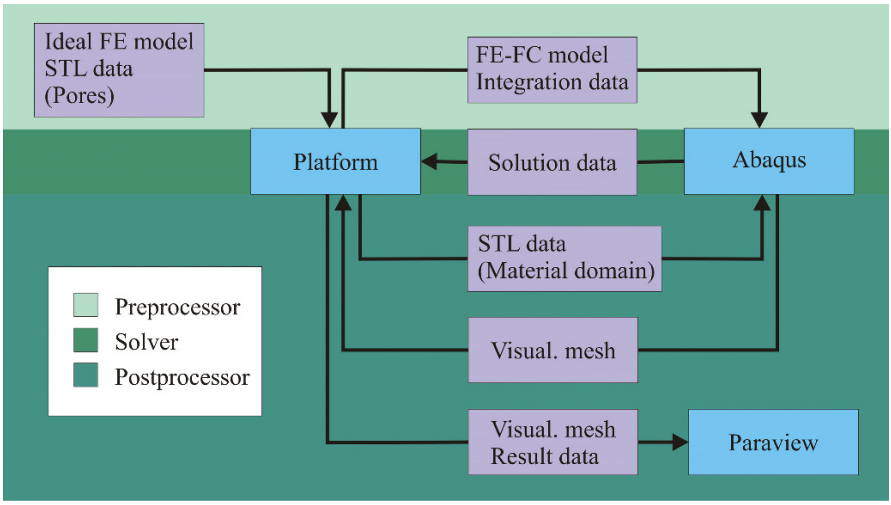

Fig. 14.4: Flow chart of the developed software platform

by finite cells. In general, as mentioned in Sect. 14.2, the expanded domain, here represented by the ideal die-cast part, can be discretized with cells. According to the adaptive numerical integration a distinction of two cases has to be considered: (i) the integration point is in the physical region and (ii) the integration point is in the fictitious domain. The numerical integration of cells completely located in the real domain ($\alpha = 1.0$) are treated as in standard finite elements. Cells, which are completely located in the fictitious domain ($\alpha = 0.0$), are removed from the model, which results in a lower effort in solving the system of equations. Only those finite cells have to be treated separately, whose domain contains the boundary of the fictitious domain, i.e. the material discontinuity Eq. (14.9). The resolution of this discontinuity in the numerical integration, controllable by the subdivision level k, has to be fine enough to reduce the integration error sufficiently.

For the sake of clarity, the finite elements belonging to the real domain do not have to be replaced by finite cells, since the numerical treatment of cells and elements is identical. These elements can be kept. The resulting FE-FC model does not differ in a numerical sense from the corresponding pure FC model.

The usage of the platform is tied to the condition, that the initial FE mesh has to be either hexahedral or tetrahedral. Due to the numerical accuracy a hexahedral mesh is to be preferred. In industrial application the geometry of a part is in general very complex. Therefore, most existing meshes are tetrahedral meshes, which are simpler to create. Using compatible finite cells the FE-FC model is established with regard to the initial FE model. The hybrid model and the data set for numerical integration (integration weights and points) of the cells given in an appropriate format are transferred via the software platform to a commercial FE tool, such as Abaqus. In Abaqus for instance, the possibility of applying user-defined subroutines (UEL

subroutines) is used to incorporate the special FCM part, which is needed to create and to solve the overall global system of equations.

The postprocessor of the software platform deals with the subsequent treatment of the vector of unknowns, i.e. the displacement at all nodes of the FE-FC mesh. These solution data are transferred to the software platform. In combination with the previously saved FE-FC model it is possible to calculate the displacements, strains and stresses at any point. For the purpose of visualizing those quantities on the FE-FC point grid a problem occurs, since points of the grid lie in the fictitious domain, which in case of representing a pore causes visualization artifacts. For this reason a grid of points is created, where all the points belong to a body-fitted mesh, the so called visualization mesh. The displacements, strains and stresses are calculated at the points of the visualization mesh by using the data from the FC-FE solution. In order to generate the visualization mesh the surface triangulation based on the FE model of the ideal die-cast part in combination with the STL data set of the pores is transferred to Abaqus and a mesh consisting of 4-node tetrahedra is created. Alternatively, the surface triangulation and its grid of points can be used for the visualization (see Fig. 14.5).

The actual visualization of strains and stresses is performed by using a data interface to the open source software ParaView. Executing ParaView and transferring the calculated results in an appropriate format provides the opportunity to an interactive evaluation of the displacements, strains and stresses.

14.4 Trouble Shooting the STL Data Set

First used in stereolithography CAD software nowadays the STL format is supported by almost every CAD software. The file format can be either Ascii or binary. As mentioned in Sect. 14.3 a STL data set is used in the preprocessor of the developed platform. This data set contains in the case of die-cast parts the pore morphology

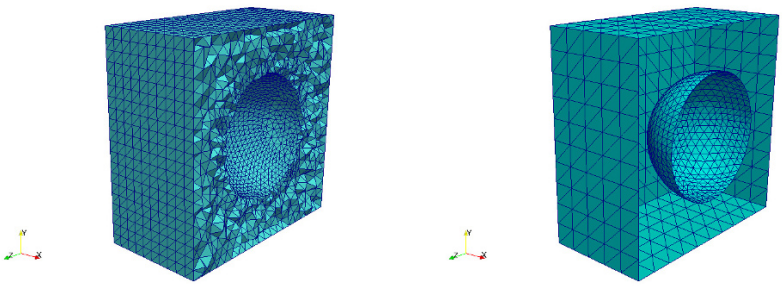

Fig. 14.5: Samples of visualization meshes: 3D tetrahedral mesh (left) and a surface triangulation mesh (right)

in form of a surface triangulation described by normals and point locations. The simplicity of the STL format using unstructured triangular facets often causes errors in the 3D meshing procedure. Overlapping of facets, incorrect normal directions, unclosed surface descriptions, etc. are not prevented by the format. Also closed surface triangulations can be connected to each other, as for instance by a line segment or a point (see Figs. 14.6 and 14.7), which complicates the unique identification of surface objects. Therefore, a mesh repair or a remeshing procedure is absolutely essential for FEM or FCM applications. However, this is a highly complex issue and topic of several publications (Bechet et al, 2002; Attene, 2014).

The repair mechanisms for STL data included in the software platform is still under development; a reorienting of the normals of facets is already included.

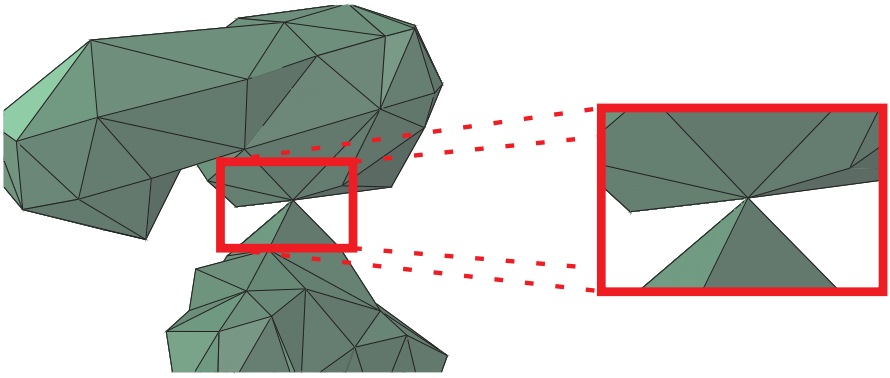

Fig. 14.6: Problems of identifying pores: Closed surface triangulations of pores connected to each other by a point

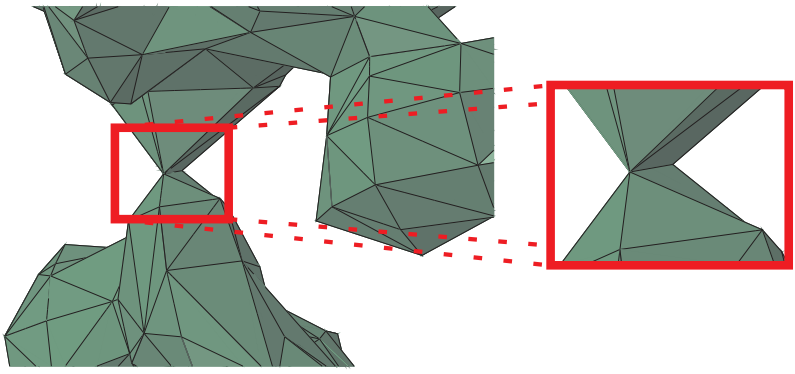

Fig. 14.7: Problems of identifying pores: Closed surface triangulations of pores connected to each other by a line segment

14.5 Verification of the Software Platform

In this section the developed platform is tested with help of some academic test cases. The objective of these investigations is to demonstrate the capability of the developed software platform of performing the complete analysis process.

The first example deals with a cube ($a = 10\,\mathrm{m}$), in which a centrally located ellipsoidal pore is embedded. The material is aluminium (see Table 14.1). A tensile load $P = 100\,\mathrm{N/m^2}$ is applied on the surface of the cube normal to the positive z-direction (see Fig. 14.8). On the opposite surface the displacements in z-direction are constrained to zero. In addition the displacements in x- and y-direction are also constrained to zero at two edges of this surface, respectively. These boundary conditions ensure enabled transverse contraction.

In order to verify the calculated quantities by using the developed software platform a reference FE analysis (Abaqus) is performed. The applied body-fitted FE model consists of 180325 tetrahedral elements (764424 DOFs) of second polynomial order (10-node tetrahedral elements; see Fig. 14.9) and is used to evaluate the computations. In comparison, the FE-FC model is based on a $25 \times 25 \times 25$ hexahedral FE mesh (204828 DOFs). Both simulations employ elements with an identical polynomial order. The subdivision level was set to $k = 3$.

Figures 14.10 and 14.11 show some results related to the developed software platform and to the purely Abaqus-based simulations, respectively. The depicted results are the displacement magnitudes (left side of the figures) and the von Mises stresses (right side of the figures). Due to the boundary conditions we can observe a band of stress concentrations at the surface of the ellipsoidal pore. It can be summarized, that the results of both analyses are in very good agreement.

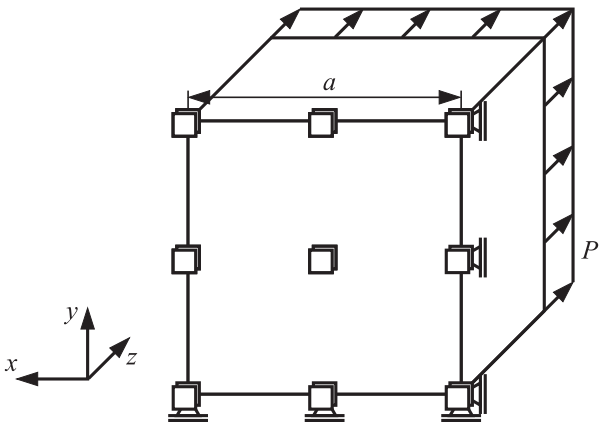

Fig. 14.8: Model definition: Boundary conditions, loads and dimensions

Table 14.1: Material properties

Material	Young's modulus [N/mm^2]	Poisson's ratio
Aluminium	70000	0.33

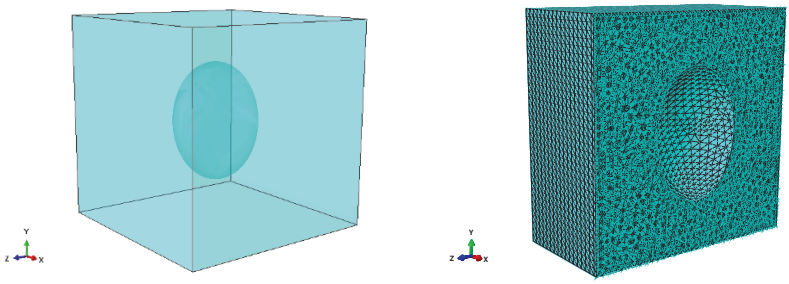

Fig. 14.9: Geometrical model of a cube with a centrally embedded ellipsoidal pore (left) and a sectional view of the corresponding FE model with a body-fitted finite element mesh

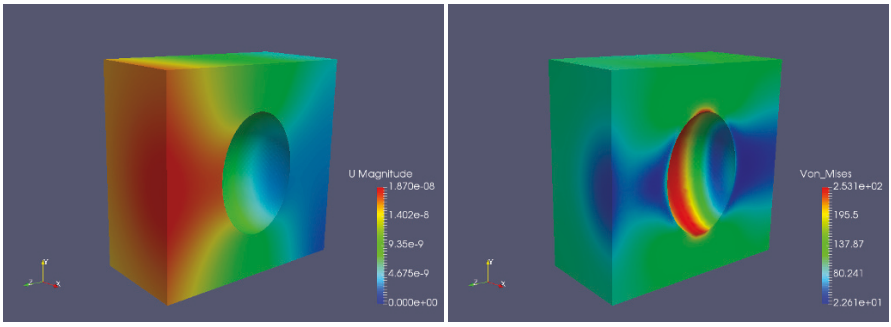

Fig. 14.10: Displacement magnitudes and von Mises stresses calculated with help of the developed software platform and a coarse FE-FC mesh of $25 \times 25 \times 25$ hexahedral elements

Next we consider an example with more than one inclusion. As shown in Fig. 14.12 a cube ($a = 10\,\mathrm{m}$) with four randomly distributed embedded ellipsoidal pores is investigated. Note that, all pores have different volumes and sizes. As in the previous example a body-fitted FE model (Abaqus) is used as reference model. The model consists of 300864 tetrahedral elements (1263081 DOFs) with a polynomial order of two. The FE-FC model is again based on a $25 \times 25 \times 25$ hexahedral FE mesh (204828

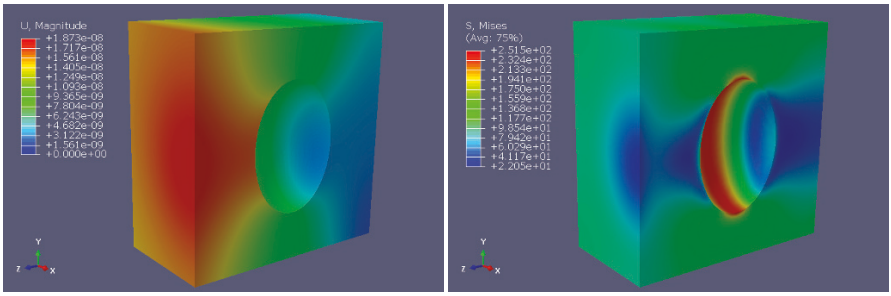

Fig. 14.11: Displacement magnitude and von Mises stresses calculated with the help of a body-fitted finite element mesh

DOFs) with an identical polynomial order. The integration subdivision level is set to $k = 4$.

In Figs. 14.13 and 14.14 the results related to the developed software platform and to the pure Abaqus model are shown, respectively. While the displacement magnitudes are in good agreement the von Mises stresses show some small differences, with a maximum value of about 6%. Nevertheless it has to be pointed out, that the model related the developed software platform only uses almost one twentieth of the element number of the reference model.

14.6 Summary and Outlook

The current paper deals with the development of a software platform using the FCM and the STL format in order to calculate displacements, strains and stresses of die-cast parts. The platform contains a complete flow chart of the analysis. The ideal

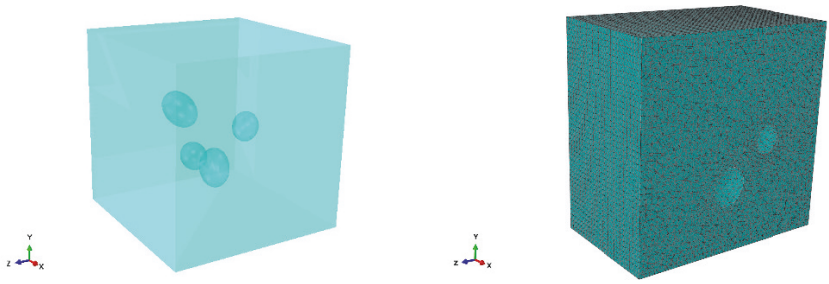

Fig. 14.12: Geometrical model of a cube with four randomly distributed embedded ellipsoidal pores and a sectional view of the corresponding FE model with a body-fitted finite element mesh

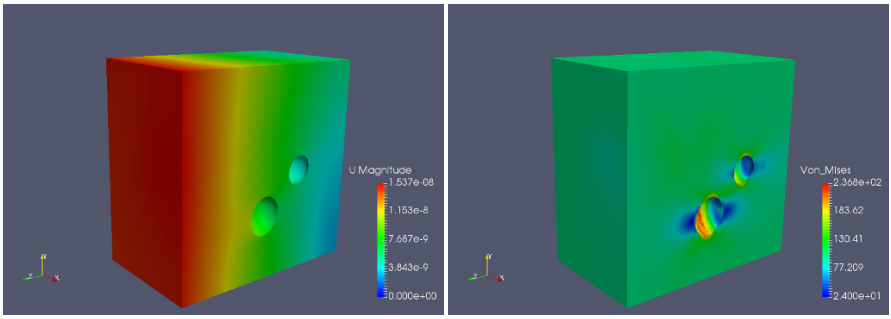

Fig. 14.13: Displacement magnitudes and von Mises stresses calculated with the developed platform

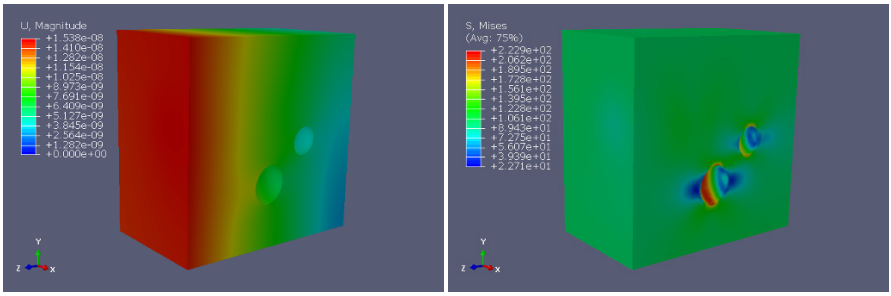

Fig. 14.14: Displacement magnitudes and von Mises stresses calculated with Abaqus

geometry given in form of a FE model and the pore morphology given in the STL format deal as initial informations for the platform. The usage of interfaces to several software tools (Abaqus, ParaView) helps the platform to assure the capability of performing a complete analysis process. The representation of the results can be interactively performed by using ParaView, where the results are based on a point grid belonging to a visualization mesh. This visualization mesh contains either a 3D point grid related to the real geometry or a grid related to the boundary surface of the real geometry.

The platform and its flow chart is verified with the help of two academic test problems. Their results, such as displacements and stresses, calculated by the platform are compared to results of body-fitted FE models, which are used as reference. Despite of much smaller numbers of DOFs compared to the reference models they are in good agreement with the calculated quantities of the FE models.

In the future, the platform and its flow chart will be tested on real die-cast part, which contains pores lying in a critical region of the part. Also improvements according to the trouble shootings with the STL format will be included in the platform.

Acknowledgements The authors gratefully acknowledge the support provided by the European Regional Development Fund (German: Europäischer Fonds für regionale Entwicklung–EFRE) and the Investitionsbank Saxony-Anhalt related to the project number ZS/2016/04/78125.

References

Ambos E, Anders U, Schalk S, Bullick M, Reinhart C, Matzen HU, Besser W (2013a) Gussteilprüfung auf einem neuen Niveau: Neue Ergebnisse über den Einsatz schneller Computertomografen in Druckgiessereien. Giesserei Erfahrungsaustausch 11/12:8–15

Ambos E, Besser W, Teuber S, Brunke O, Neuber D, Stuke I, Lux H (2013b) Einsatz der schnellen Computertomographie zur Porositätsbewertung an Druckgussteilen. Giesserei-Rundschau 60:14–22

Attene M (2014) Direct repair of self-intersecting meshes. Graphical Models 76:658–668

Bathe KJ (2002) Finite-Elemente-Methoden. Springer-Verlag

Bechet E, Cuilliere JC, Trochu F (2002) Generation of a finite element MESH from stereolithography (STL) files. Computer-Aided Design 34:1–17

Duczek S (2014) Higher Order Finite Elements and the Fictitious Domain Concept for Wave Propagation Analysis. VDI Fortschritt-Berichte Reihe 20 Nr. 458, URL `http://edoc2.bibliothek.uni-halle.de/urn/urn:nbn:de:gbv:ma9:1-5434`

Duczek S, Berger H, Ambos E, Gabbert U (2015) Eine neue Methode zur Berücksichtigung des Einflusses der Porosität in Al-Druckgussteilen auf die Festigkeit - Ein Beitrag zum Leichtbau. Gießerei-Rundschau 62:222–227

Duczek S, Duvigneau F, Gabbert U (2016) The finite cell method for tetrahedral meshes. Finite Elements in Analysis and Design 121:18–32

Düster A, Parvizian J, Yang Z, Rank E (2008) The finite cell method for three-dimensional problems of solid mechanics. Computational Methods in Applied Mechanics and Engineering 197:3768–3782

Oberdorfer B, Habe D, Kaschnitz E (2014) Bestimmung der Porosität in Al-Gussstücken mittels CT und ihres Einflusses auf die Festigkeitseigenschaften. Giesserei-Rundschau 61:138–141

Parvizian J, Düster A, Rank E (2007) Finite cell method: h- and p-extension for embedded domain problems in solid mechanics. Computational Methods in Applied Mechanics and Engineering 41:121–133

Ramière I, Angot P, Belliard M (2007) A fictitious domain approach with spread interface for elliptic problems with general boundary conditions. Computational Methods in Applied Mechanics and Engineering 196:766–781

Rank E, Düster A, Schillinger D, Yang Z (2009) The finite cell method: High order simulation of complex structures without meshing. In: Yuan Y, Cui JZ, Mang H (eds) Computational Structural Engineering, Springer Science+Business Media B.V.

Rehse C, Schmicker D, Maaß A, Bähr R (2013) Ein Bewertungskonzept für computertomographisch ermittelte Porositäten in Gussteilen hinsichtlich ihrer Auswirkung auf die lokale Beanspruchbarkeit des Bauteils. Giesserei-Rundschau 60:106–110

Saul'ev VK (1963) On solution of some boundary value problems on high performance computers by fictitious domain method. Siberian Mathematical Journal 4:912–925

Zander N, Kollmannsberger S, Ruess M, Yosibash Z, Rank E (2012) The finite cell method for linear thermoelasticity. Computers and Mathematics with Application 64:3527–3541

Zienkiewicz OC, Taylor RL (2000) The Finite Element Method - Volume 2: Solid Mechanics. Butterworth-Heinemann